Journal of Geomatics Science and Technology

Very High Resolution Parametric and Non- Parametric Sartomography Methods for Monitoring Urban Areas Structures

S. Adeli[1], M. Akhoondzadeh[*2], S. Zakeri[1]

1- MSc student at School of Surveying and Geospatial Engineering, College of Engineering, University of Tehran, Tehran, Iran
{sarina.adeli, salar.zakeri}@ut.ac.ir

2- Assistance professor at School of Surveying and Geospatial Engineering, College of Engineering, University of Tehran, Tehran, Iran
makhonz@ut.ac.ir

(Received: February 2018, Accepted: August 2018)

Abstract

Synthetic Aperture Radar (SAR) is the only way to evaluate deformation of the Earth's surface from space on the order of centimeters and millimeters due to its coherent nature and short wavelengths. Hence, by this means the long term risk monitoring and security are performed as precisely as possible. Traditional SAR imaging delivers a projection of the 3-D object to the two dimensional (2-D) azimuth-range (*x*-*r*) plane. Due to the side looking geometry of SAR sensors problems like foreshortening, layover and shadow should be dealt with. For overcoming the problem of layover in high urban environment different SARtomography methods are developed. The aim of SARtomography methods are not only overcoming layover problem but unambiguous 3-D and 4-D (space-time) dynamic map of the city can be achieved. The assumption, made by the classical interferometric techniques (i.e.: PSI), the present of a single scatterer per pixel, neglects the fact of occurrence of mulitiple scatterers. For instance PSI initial assumption is the presence of single sactterer in each azimuth-cell range. However, this assumption is not plausible in a high rise urban environment where suffers from the presence of multiple scatter. Furthermore, by the advent of Very High Resolution sensors like Cosmos-Skymed (1,2,3) constellation SARtomography is revolutionized. Needless to say that due to the very high resolution of the images (up to 1m resolution), precise shape and deformation of each individual building can be obtained. Nonetheless, it has to be noted that the increasingly impact of layover on new generation of VHR sensors. To this end several practical SARtomography methods such as first order model and Non Linear least Square (NLS) are introduced. This paper has presented the capacity of the new class of VHR spaceborne SAR systems, like COSMO-Skymed, for TomoSAR processing in high urban environment. However, particular problems related to the side looking geometry of SAR has proved to be more obvious comparing to the previous generation of high resolution sensors (10 m resolution): Layover is one of them. The main aim of this paper is at comparing SARtomography methods and their advantage and disadvantage to the older version of SAR methods like PSI for monitoring high urban environment. The project has been implemented on Very High Resolution (VHR) Cosmo-skymed Stripmap mode (up to 3m azimuth-range resolution) images from Astana-Kazakhstan. Like PSI, TomoSAR benefits greatly from the high resolution of Cosmo-skymed data, as the density of coherent pixels and the signal-to-clutter ratio increase significantly with resolution. The results reveal that the number of permanent scatterers found by NLS and first order model are far more than PS method which indicate the superiority of these methods in overcoming the layover problem in high environment urban areas comparing to the PSI; Besides, the mean deformation velocity, height and coherence of every scatterer were obtained by SARtomographic methods are compared with PSI. As it comes to tomographic processing methods different factors must be taken into account such as the accuracy in estimating the heights, computational cost and the model order selection. Results indicate that the first order method has low computational cost but it suffers severely from side-lobes on the other hand the computational cost of NLSM is very high but it is an accurate method as long as the correct model order is selected. SARTomography proved to be an efficient method for detecting multiple scattrers and layover removal in high urban environment.

Key Words: Synthetic Aperture Radar (SAR), SARTomography, Persistent Scatterer, VHR Cosmo-skymed data, Multidimensional SAR Processing

[*] Corresponding Author

1. Introduction

By the emerge of Synthetic Aperture Radar (SAR) in remote sensing society the increasing application of SAR system for performing the long term risk monitoring and security is being possible[1,2]. Advanced introfermetric SAR would allow us to retrieved 3-D shape and deformation of each building. Across track Introferometric SAR (InSAR) combine two or more complex-valued SAR images to obtain phase differences. This phase difference is associated to topography of the surface which can be used to generate digital elevation models (DEMs)[3,4]. Hence, InSAR methods allow us to access third dimension. Extended version of InSAR called D-InSAR can be used to obtain precise movement in range direction. Needless to say that the accuracy of InSAR and D-InSAR are limited by the temporal decorrelation of the surface and by electromagnetic path delay variations in the troposphere. Due to the problems caused by these two methods averaging of multiple introferograms has been introduced. Averaging the multiple introferograms play a tremendous role for diminishing path delay and troposphere error but in turn it will reduces the temporal resolution. Persistent Scatterer Interferometry (PSI) was introduced in 1999 [5] as a methodology for long-term monitoring of subsidence, preferably in urban Environments. Unlike D-InSAR PSI's goal is to analyze multipass interferometric stacks on a fine scale; for instance scattering mechanisms which are very compact and stable (in the electromagnetic response) and therefore recognized by a high temporal correlation degree. Usually 40-70 interferograms data sets taken from same area and approximately same orbit required. PSI tries to separate the phase contributions including elevation of the point, deformation parameter, orbit errors and tropospheric water vapor delay[6 , 7]. An astonishing extension of PSI through DInSAR techniques is obtained by SqueeSAR [8]. SqueeSAR manipulate the influence of target decorrelation in order to overcome the shortages over non-urban areas. Additionally the Small Baseline Subset (SBAS), and the Coherent Point Target (CPT) analysis Techniques, are presently routinely applied to the monitoring of surface deformations stimulated by natural hazards, such as landslides, earthquakes, and volcanic activities [2]. Therefore, providing us a precious tool for civil protection use in all the phases of the risk management. The assumption, made by the classical interferometric techniques, a single scatterer per pixel, neglects the presence of double scatterers. It shouldn't be neglected that, the problem of multiple scattereres including pixels have more than one scatterers in every azimuth-range pixels cannot be solved, since PSI initial assumption is the presence of single sactterer in each azimuth-cell range. Nonetheless, this assumption is not plausible in a high rise urban environment where suffers from the presence of multiple scatter [9]. Consequently, it is more possible to multiple scatteres project in the same azimuth-range pixel. Traditional SAR imaging delivers a projection of the 3-D object to the two dimensional (2-D) azimuth-range (x-r) plane[10]. Due to the side-looking geometry, this projection stimulates challenges like foreshortening, layover and shadowing, especially when we face volumetric scatterers and man-made object in urban areas [11].

Therefore, the side looking geometry of SAR sensors should not be overlooked. In the presence of a vertical structure, such as a building, the radar signal is affected by layover between the ground, the façade, and possibly the roof [12]. The layover can be overcame by using SARtomography methods still the foreshortening is a big challenged. To be more specific, with the advent of new SAR sensors, such as the German TerraSAR-X/TanDEM-X and the Italian COSMO-Skymed satellites, SAR remote sensing has been revolutionized. These satellites deliver SAR data with a very high spatial resolution of up to 1 m. These satellites provide us the opportunity to use precise SAR images for 3-D, 4-D (space-time) of urban structures and individual buildings from space[13]. Needless to say that they have great geometric accuracy. Moreover, the higher the resolution the higher the density of permanent sactterers in image, since the signal to noise ratio increases with the resolution and the ability of SAR image in detecting the permanent scatteres improves due to the high geometric resolution and density of coherent pixels. Nonetheless we have to consider the increasing impact of layover stimulates by the very high resolution new generation of sensors. The covered area is hugely large in images taken by these sensors. In other word the higher the geometry resolution the more layover effect would be emerge [9]. To this end several SARtomography approaches has been established for instance Spectral estimation methods including :conventional Beem Forming(BF)[14], Singular Value Decomposition (SVD)[15], adaptive beamforming (capon)[16], Multiple Signal Classification(MUSIC), Nonlinear Least Squares (NLS)[17] and M-RELAX. Every SARtomography method needs to preserve the azimuth-range resolution, enhance the elevation resolution and retrieval linear motion [18]. The main goal of SARtomography is real and unambiguous 3-D SAR imaging. Tomosar has to deal with sparse and irregular sampling in elevation[19 , 9]. Hence its momentous importance of Tomosar is overcoming layover problem and access the third dimension with no ambiguity. D-Tomosar (4-D, space-time), also take advantage of the strength of PS and

TomoSAR simultaneously [19]. Not only does the shape of building retrieved but also we can access the deformation of each individual building.

The main goal of this paper is at indicating the potential of the new class of VHR spaceborne SAR systems for TomoSAR in high urban environment. In this experiment the potential capability of PS approach and two TomoSAR methods has been acknowledged. Moreover, their weakness and strength are evaluated. Two practical TomoSAR method are implemented on very high resolution Cosmo-skymed data. The precision of the PS, First-order model and NLS method are compared by the detected number of scatteres, their coherences and velocities. Also, 4-D accurate map of the area is achieved.

In Section 2 methodologies are presented. In Section 3 the experimental results are introduce and finally in Section 4 a brief discussion and conclusions for further research are available.

2. METHODOLOGY

The standard spectral estimation methods can be classified as *non-parametric* methods (most of the classic methods) and *parametric* methods (most of the modern methods). The former needs an initial assumption about the number of scatteres in each azimuth-cell pixel. Conversely, the latter works under the condition that the method specifies the number of scatterer in each cell. As it can be seen in Flowchart 1. Non-parametric methods require the model order selection step. Model of surface without layover is the final result of SARTomography. Additionaly, methods can be classified as single-looking and multi-looking. Generally, multi-looking methods obtain higher SNR and SR in elevation by foregoing resolution in azimuth and range. However, in SARtomography methods it's more efficent to maintain the azimuth-range resolution.

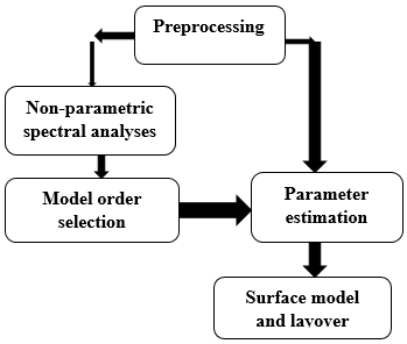

Flowchart 1. Processing sequence of Tomographic SAR data stacks

2.1. PERSISTENT SCATTERERS

Following the PS approach presented in [20 , 21] data are first coregistered on a unique master and N differential interferograms between all SAR images and the master are computed using a reference Digital Elevation Model (DEM) of the area. In general, the PS carries out two steps: 1) Displacement first inversion : The estimated linear model (velocity + residual height) will be subtracted from all dint files. From the residual, the atmosphere will be estimated containing the noise and non-linear target motion. 2) Displacement second inversion: Atmosphere estimation on differential interferograms.

2.2. First-order model

This method can be considered as an extension of the PS method. However, instead of looking for only one dominant scatterer in each individual azimuth-range cell the Fourier based method tries to retrieve a continues coherence along the elevation [17]. PS works under the premise that the time and look angle of acquisition of the SAR data does not affect the value of the amplitude of the backscattered signal from the target. As it can be seen in Figure 1 the geometry of the problem under study is shown. For a target without motion the phase value of the backscattered signal from the target P of the i_{th} interferogram could be modeled as the following:

$$\phi(P,t_i) = \mu(\mathrm{P},\mathrm{t}_i) + C^i_{DEM}\varepsilon(P) + \eta(P,t_i),\ \mathrm{i}=1,\ldots,\mathrm{N} \qquad (1)$$

Where t is the temporal baseline of the i_{th} interferogram, $\mu(\mathrm{P},\mathrm{t}_i)$ is the phase caused by noise and atmospheric leakage, $\varepsilon(P)$ is the elevation of the target from the reference DEM, C^i_{DEM} is computed according to the normal baseline B_i of the interferogram $\eta(P,t_i)$ is the phase caused by the motion of the target.

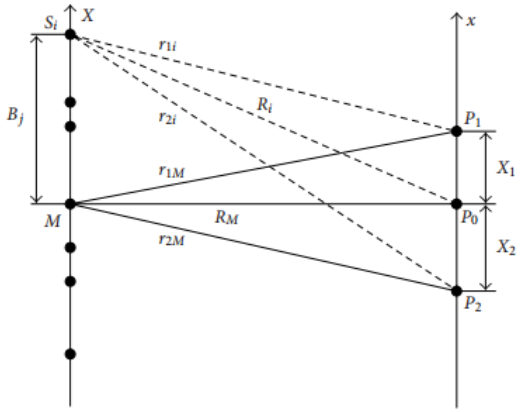

Figure 1. Geometrical schematization of the problem under study. An N-sensor array receives signal from two (or more) sources.

$$C^i_{DEM} = \frac{4\pi B_i}{\lambda R\sin\theta} \equiv \frac{A^i_{DEM}}{\sin\theta} \qquad (2)$$

Where R is the distance of the sensor from target and λ is the wave length of the sensor. Time series analysis of the first term in (1) should reflect target motion.in the following a constant-velocity model will be

$$\mu(\mathrm{P},\mathrm{t}_i)=\frac{4\pi}{\lambda}v(\mathrm{p})\,\mathrm{t}_i=C_v^i v(\mathrm{p}) \tag{3}$$

where v(p) is the velocity of the scattering centre within the resolution cell. From the above considerations, we can finally write the model of the interferometric phase of each interferogram

$$\phi(P,t_i)=C_v^i\,\mathrm{v}(P)+C_{DEM}^i\varepsilon(P)+\eta(P,t_i),\ \text{for i=1,…N} \tag{4}$$

adopted As explained in [20] by maximizing the phase coherence function the unknown parameter of $\varepsilon(P)$ could be found.

$$\gamma_I(P)=\frac{1}{N}\left|\sum_{i=1}^{N}e^{j\phi data,i}\,e^{-j\phi \mathrm{model},i}\right|, \tag{5}$$

2.3. Non-linear Least Square Method (NLSM)

We will now discuss the case of multiple scatterers within resolution cell. This yields a second-order model [22]. The Non-Linear least Square Method (NLSM) is a parametric method therefor it does not needs a prior knowledge about the number of interfering scatterers located in a single azimuth-range cell. Here we implement the Nonlinear Least Squares Method (NLSM) offered in [23], due to its effectiveness and robustness in most cases. For our purpose which is to assess the capability of NLSM to separate the backscatter from the two tall buildings. The model order is set to two. As explained in [17] the permanent scatter method could be extended in to higher order models.

As it can be seen in Figure 2. M is the master antenna, S the slave. Based on Figure 2 following equation can be derived.

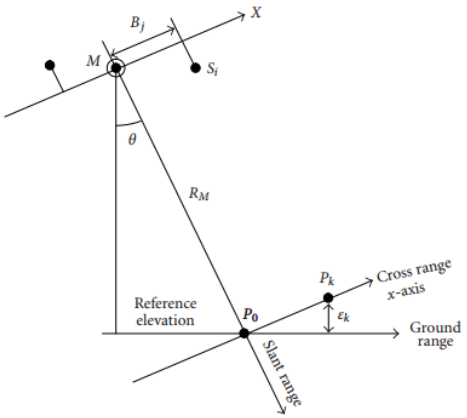

Figure 2. SAR acquisition geometry. M is the master antenna, S the slave. Parallel baseline components do not impact the mathematical modelling for phase variations. $P0$ represents the reference DEM for the pixel under analysis. P is the dominant scattering-centre within the resolution cell.

The complex signal received by *ith* sensor can be modeled as:

$$s_i=z_1e^{j(4\pi/\lambda)r(B_i,t_i,x_1)}+z_2e^{j(4\pi/\lambda)r(B_i,t_i,x_2)}, \tag{6}$$

From figure 3 we have (since the distance between sensor and earth is too long this approximation can be considered plausible):

$$r_{kM}\cong R_M+\frac{x_k^2}{2R_M},\ \text{k=1,2} \tag{7}$$

As discussed in [17] this equation can be achieved:

$$y_i=\beta_1e^{j(A_{DEM}^i x_1-C_v^i v)}+\beta_2e^{j(A_{DEM}^i x_2-C_v^i v)},\text{i=1,…,N} \tag{8}$$

Since $x=\varepsilon/\sin\theta$ we can write previous equation as this:

$$y_1=\beta_1e^{j(C_{DEM}^i\varepsilon_1-C_v^i v)}+\beta_2e^{j(C_{DEM}^i\varepsilon_2-C_v^i v)} \tag{9}$$

Once we conclude this we have to solve inverse problem. This has been discussed in [17] comprehensively however we explain it briefly in here. The cost function which should be minimum in NLSM is:

$$J=[\mathrm{y}-x(\theta)]^H[\mathrm{y}-x(\theta)] \tag{10}$$

As discussed in [17] we will have

$$J=\sum_{i=1}^{N}\left|y_i-\sum_{k=1}^{n}\alpha_k e^{j(\omega_k m+\varphi_k)}\right|^2,$$
$$B=\begin{pmatrix}e^{j(C_{DEM}^1\varepsilon_1} & e^{j(C_{DEM}^1\varepsilon_2}\\ \vdots & \vdots\\ e^{j(C_{DEM}^N\varepsilon_1} & e^{j(C_{DEM}^N\varepsilon_2}\end{pmatrix} \tag{11}$$

Then by maximizing**:**

$$\hat{\omega}=\arg\max\left[Y^H B(B^H B)^{-1}B^H Y\right] \tag{12}$$

We could then finnaly obtain the relative heights of the scatteres and then the coherence:

$$\hat{y}_i=\hat{\beta}_1e^{j(C_{DEM}^i\varepsilon_1-C_v^i v)}+\hat{\beta}_2e^{j(C_{DEM}^i\varepsilon_2-C_v^i v)} \tag{13}$$

$$\gamma_{II}(P)=\frac{1}{N}\left|\sum_{i=1}^{N}e^{j\phi data,i}e^{-j\angle\tilde{\gamma}_i}\right| \tag{14}$$

Every initial steps for preprocessing the real data is shown in the flowchart 2. First SAR data stacks with SLC format imported in SARSCAPE software in order to generate connection graphs and

diffrenetial inteferograms. With dint files PS processing can be done and coherence, velocity and height of each scatterer obtained. For the sake of SARTomography experiment dint files imported to IDL for coding and obtaining results. SARtomography prooved to be an efficent method for estimating number of multiple scattere beside it has the capability to obtain coherence,velocity and topography estimation.

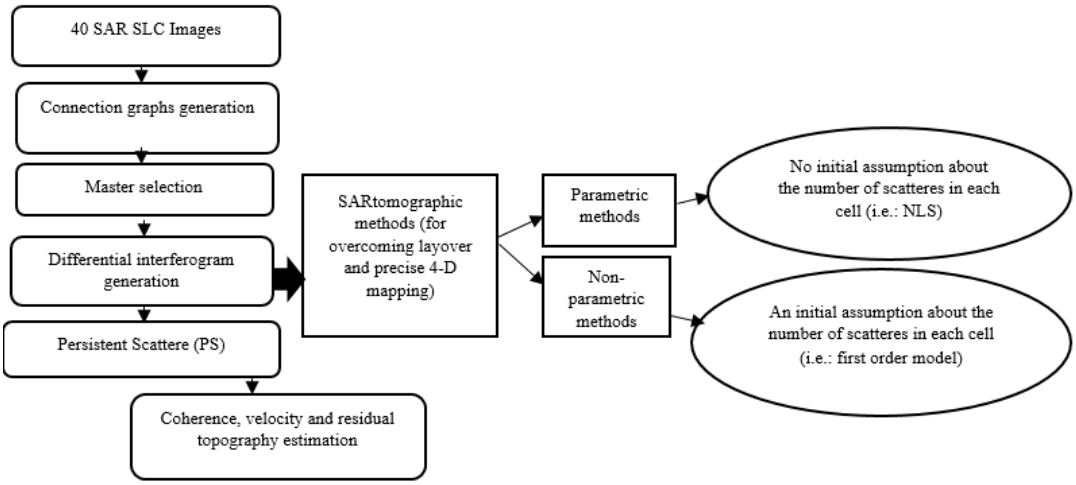

Flowchart 2.The workflow of preprocessing of PS and SARtomography parametric and non-parametric metho

3. EXPERIMENTAL RESULTS

3.1. Data Set

The data set is used in this research is 41 very high resolution Cosmo-skymed images from Astana-Kazakhstan in three years period. The selected area is an urban area containing several tall buildings, a likely position for occurrence of layover. From the stack of 41 images 40 differential interferograms were created. Characteristic of the images used in this research is indicated in Table 1. The images are in stripmap mode and provide up to 3m resolution in each azimuth-cell resolution. Since the acquired scene is 40*40 kilometer we focus on specific buildings in Astana named Lagrange Education. google earth visualization of the are has been prepared in order to ease for envisaging the spot in Figure 3. the scene of the area with with its coordinates (latitude: $51^{\circ}40'33''$N longitude: $72^{\circ}47'10''$E) is presented in Figure 3. Additionally, in Figure 4 the image of the area aquired by the sensor can be seen. The whiter spots are the probable area for accuring the layover and ambiguity due to the fact they might be the place for accuring multiple scatterer. Almost all the images are acquired with the minimum repeat cycle of 11 days, from January 2011 to December 2014. The polarization of the images is single polarize H-H. Low incident angle is being preferred in order to reduce the shadowing effect.

Acquisition Mode	STRIPMAP HIMAGE
Range resolution (m)	3
Azimuth resolution (m)	3
Swath width (km)	40
Scene length (km)	40
Polarization	H-H
Revisit time(Days)	11
Incidence angle (degree)	22-37

Table1. COSMO-SkyMed product details in this research

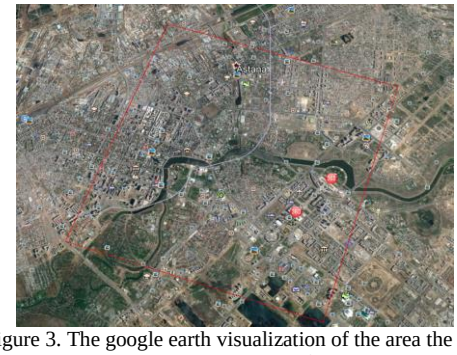

Figure 3. The google earth visualization of the area the red square distinguish the 40*40km scene frome sorrunding area (latitude: $51^{\circ}40'33''$N longitude: $72^{\circ}47'10''$E)

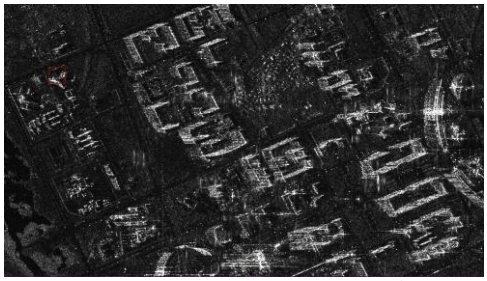

Figure 4. Cosmo-skymed amplitude image of the area

The extremely high resolving capabilities of the Strimpap Cosmo-skymed imaging that allows distinguishing floors on the façade would enable us to overcome layover as efficient as possible.

3.2. Results

For the sake of computational simplicity we crop the image and process the cropped area which contains several very tall building. In Figure 5(a) the Google Earth of the cropped area can be seen. Beside the specific range line and its interferogram has been shown in Figure 5(b) and 5(c). The initial preprocesses including time-baseline plot and time-position plot and generation of differential interferograms (dints) are undertaken in SARscape software. This functionality defines the SAR pair combination (Master and Slaves) and connection network, which is used for the generation of the multiple differential interferograms. These pairs are shown as connections in a network that links each acquisition to the Master (reference) file. Given 41 acquisitions, the available connections are 40. The Connection Graph tool allows choosing the most a-priori reliable connections. The Time-Position plot is shown in Figure 6 (a), which provides the normal distance from the Master (y axis) and the input acquisition dates (x axis). Additionally, Time-Baseline plot, which provides the normal baseline (y axis) and the input acquisition dates (x axis) has been shown in Figure 6 (b). This graph allows to better visualize the interferogram coverage for each date. At the first step we have to produce the differential interferograms (dints). Declaring that since we have 41 image scenes we have 40 dints. This dints contains phase information which is vital for the next step. The data set was calibrated for atmospheric phase components estimated via the multi-pass DInSAR approach before the tomographic processing. Once the dints were prepared we will use the PS method to access information about the shape and deformation of each individual building by time series analyzes. Afterwards two practical SARtomography methods including Fourier based and Non-linear least square (NLS) are implemented. Their results on real data and their weakness and strength are weighted.

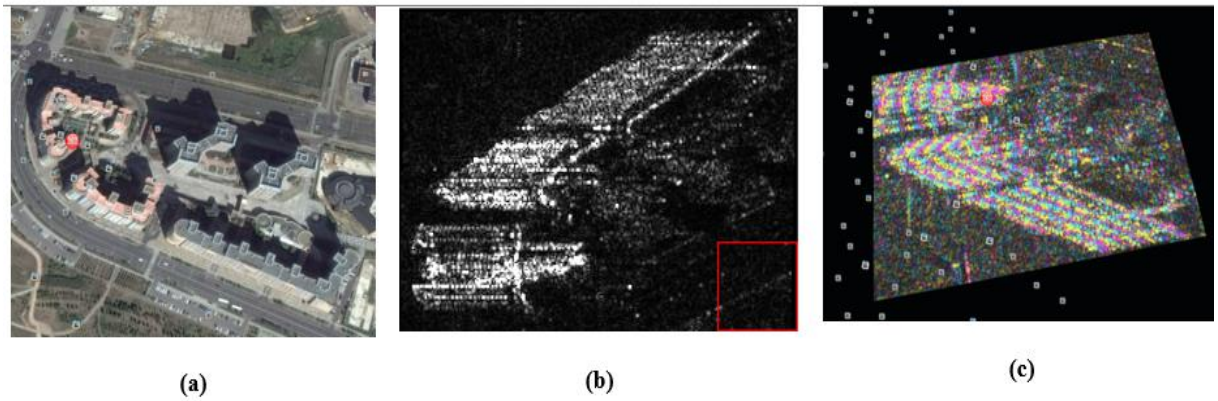

Figure 5.(a) Google earth visualization of the cropped area (Lagrange Education), (b) Cosmo-skymed crop amplitude image of the area, (c) Differential interferogram of the cropped area was projected in Google earth scene

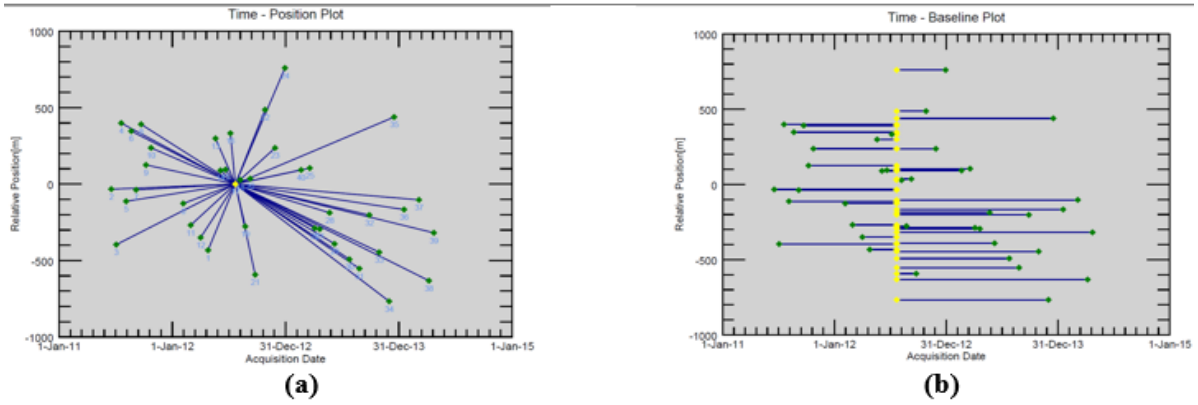

Figure 6. (a) Time-position plot of acquisitions from 2011 to 2014, (b) Time-baseline plot of acquisitions from 2011 to 2014

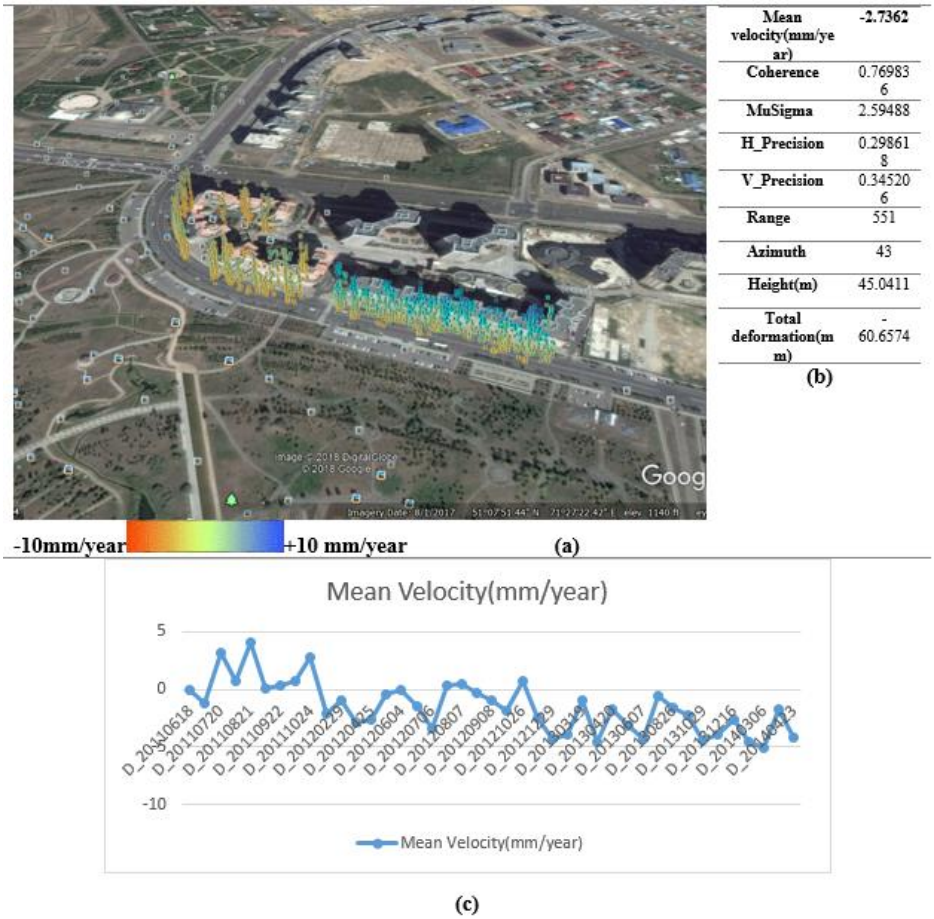

Figure 7.(a) Map of mean deformation velocity of permenant scatteres detected by PS method, (b) the specific permenent scattere characteristic with lat:51.127 and long:71.4611 coordinates, (c) mean velocity of the specific permenant scattere in 3 years period.

Permanent scatterer points are shown in Google Earth image for better visualization in Figure 7 (a). Colors correspond to the velocities of Permanent scatteres. This example presents the 3D location precision and the PS density which perfectly provides the shape of the building's front. The mean velocity map also shows an interesting phenomenon: While all the rest is stable, the roof appears moving toward the sensor at about 3 mm/year. The PS density of Cosmo-skymed allows to monitor the structural stress of buildings. This example presents the deformation (red to blue: -2mm/y to +2mm/y) which results from thermal dilation of the building's roof. PSI is applied very successfully with medium resolution SAR data from ERS-1/2 and ENVISAT/ASAR. Subsidence rate accuracies of better than 1mm/a have been reported; Nonetheless, the physical interpretation of these estimates has established to be difficult. The low resolution does not give access to details of the buildings. The PSs appear to be quite randomly distributed at a density of about 100–500 PS/km2, i.e., one PS per block of 100m x 100m to 50m x 50m. There is no guarantee that a particular building of interest is represented by a PS. It is also difficult to differentiate between the subsidence of the building itself or of the pavement surrounding the building; However, the new generation of very high resolution Cosmo-skymed data's absolutely shows the extreme potential ability of them. As it can be seen in figure 7 (b) the coherence for the specific persistent scatterer is extremely high. This can be assumed as a proof for the accuracy of the implementation. Plus, the mean velocity revealed that this area does not have huge deformation. However, the minus value for velocity indicated a subsidence deformation. The total deformation for that specific permanent scatter also shows that (~ -60 mm) this area does not suffer from land subsidence. The time series of mean velocity for the specific permenant scattere in a period bound between 2010 and 2014 can be seen in figure 7 (c). The overal behaviour of the permenent scatterer indicate a subsidence deformation in this area. Like PSI, TomoSAR benefits greatly from the high resolution of Cosmo-skymed data, as the density of coherent pixels and the signal-to-clutter ratio increase significantly with resolution. In the next step a range line where two buildings are located and hence is a possible location for layover was chosen also since the goal is to assess the capability of these methods in detecting multiple scatteres a range line was selected where the motion of scatteres is negligible. The tomographic process is applied using two methods explained above. The NLS method is a parametric method which means

that there is no initial assumption about the number of scatteres needed. Hence, this method doesn't need model order selection unlike non-parametric methods like Singular Value Decomposition (SVD). The methods are compared and their ability to improve the P.S method is inspected. The coherences and velocities of the area is obtained by P.S method and two SARtomography methods. The assumption, made by the classical interferometric techniques, of a single scatterer per pixel neglects the interference of scatterers. We therefore applied the detection scheme described (first-order model, NLS) which is able to test the presence of single and double scatterers. In Figure 8 (a), the results of first-order model algorithm are presented with the colors coded accordingly to the estimated topography. The x axis shows the range of bins (0-1000) and y axis represents the estimated height (-70,+70 m) and the colors relate to the coherency of each scatterer. It can be seen that the green areas show the almost high coherency which reveal the presence of single and double scatterer in the façade and roof of building. Figure 8(b), reveals the coherence obtained by first-order model and PS method. It be can clearly seen that from 200 to 750 range-bins there is extremely accurate match between PS and first order model coherence. In Figure 8 (c), the mean deformation velocity of PS method has been compared with First-order model. Again the approximately equal mean deformation velocity from 200 to 750 range-bins can be acknowledged. As mentioned before the area does not suffer from huge deformation, hence, the mean deformation velocities are from -3 mm/year to +3 mm/year. For the sake of simple visual imagination in figure 8 (d) we present the 3-D Google Earth height estimation which obtained by first-order model. It can be seen that although first –order model is the fast and low computational cost method but it vastly suffers from side lobs.

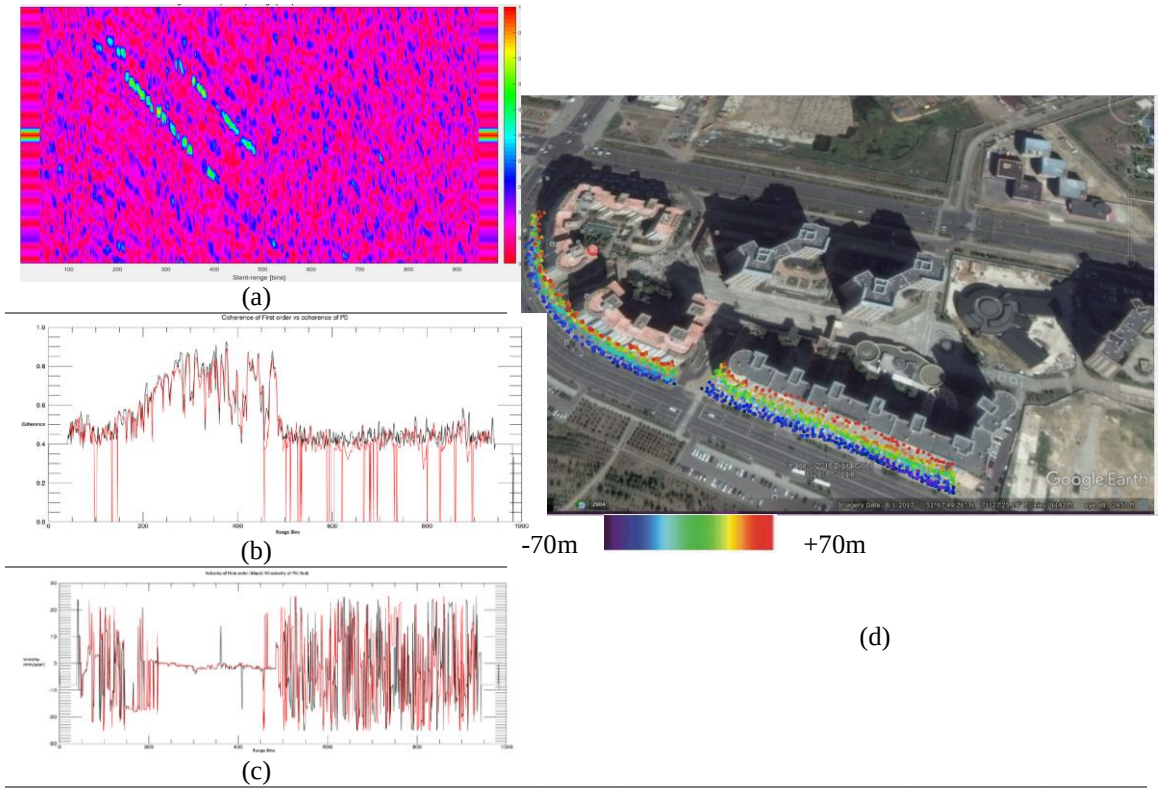

Figure 8.(a) 3-D map of single and double scatteres were found by first order model. (b) coherence of scatteres were found by first order model compared to PS method (black line:first order model,red lines:PS method).(c) velocity of scatteres were found by first order model compared to PS method (black line:first order model,red lines:PS method). (d) 3-D visualization in Google Earth environment of scatterers detected by first-order model 4-D imaging. Colors are set according to the estimated height.

In figure 9(a), like first order-model, in the NLS algorithm the X axis represents range-bins and Y axis represent the height and the color reveal that the coherence of the scatterers. As it can be acknowledged two white lines are related to the range lines where layover happened. NLSM has been accomplished to reconstruct the building structure. The momentous importance of SAR methods in identifying the scatters in shadow areas should not be neglected. Thus the low incident angle is being preferred since it can reduce the shadow effect. In Figure 9 (b), the coherence of three methods (NLSM, PS, First-order model) is compared. Again from 200 to 750 range-bins great match between these 2 algorithms is available. In Figure 9(c) the mean velocity of the scatterers were calculated by the NLSM ,are compared to PS method. Finally the Google earth visualization of the scatters were found by NLSM has been shown in Figure 9 (d). NLSM proved to be high

computational method which is so time-consuming to run the process. Nonetheless, its potential capability of detecting double scatterers should not be overlooked. The effectiveness of tomography in scatterer pair separation on this layover (distributed over several range pixels) is predominantly evident in the topography reconstruction; see the homogeneity of blue color of the ground scatterer layer and the gradation of colors on the layer corresponding to the façade. The high density of detected double scatterers that fills the lack of the single scatterers analysis should be noticed. A further confirmation of the results is provided by the shadow. As expected, no double scatterers were detected in this area. These figures show the capability of the tomographic approach to "separate" the interfering layers associated with the ground and the façade of the building.

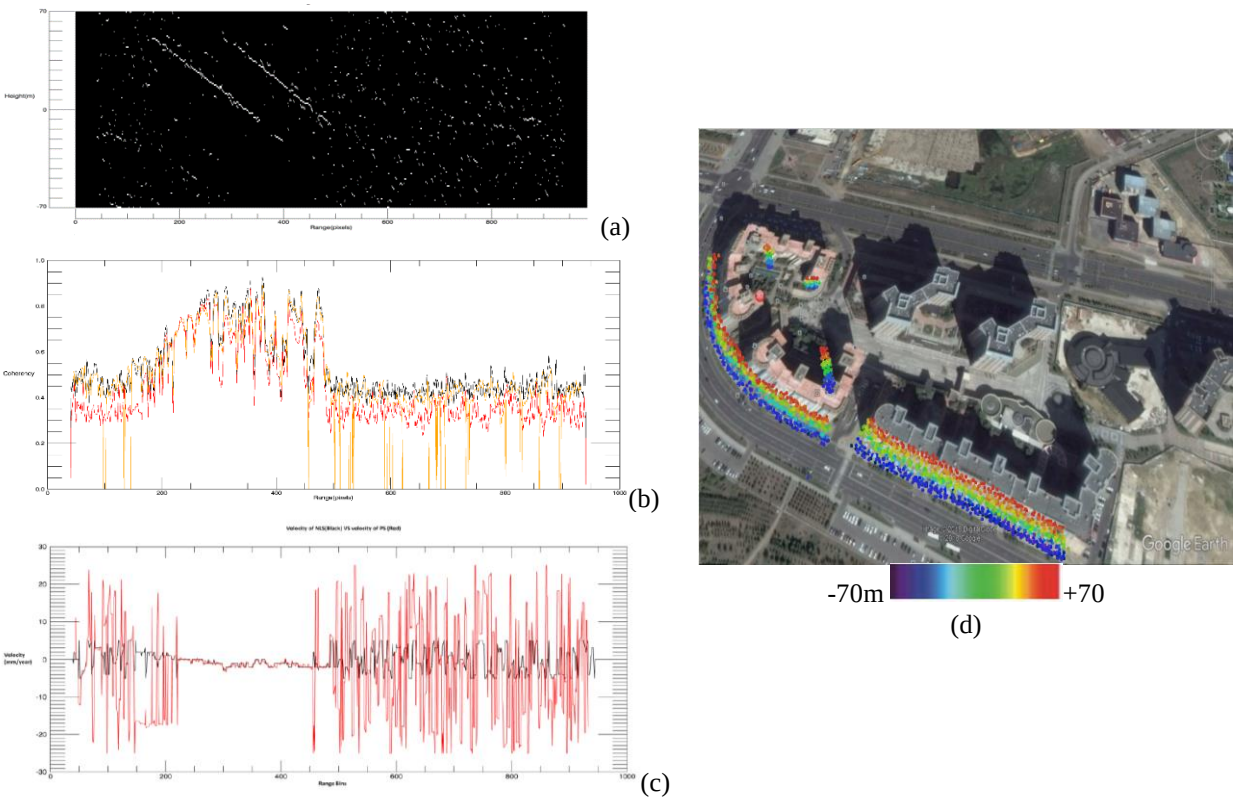

Figure 9.(a) Result of NLS for the selected range line with model order . (b) coherence of scatteres were found by NLSM compared to PS and first-order model method (Coherence of NLSM(black) – Cohrence of PS (Orange)- Coherence of Fourier-Based method(Red).(c) velocity of scatteres were found by NLSM compared to PS method (black line:first order model,red lines:PS method). (d) height estimation visualisation by NLSM method on Google Earth

4. CONCLUSIONS AND DISCUSSION

This paper presents the capacity of the new class of VHR spaceborne SAR systems, like COSMO-Skymed and TerraSAR-X, for TomoSAR processing in high urban environment; However, particular problems related to the side looking geometry of SAR has proved to be more obvious comparing to the previous generation of high resolution sensors (10m resolution): Layover is one of them. It has predominantly influenced on the images of urban environment. SARtomographic methods proved to be efficient method for overcoming the layover problem. Equally of note is the fact that the problem of shadowing and foreshortening are momentous challenges, yet the lower incident angles are being preferred for declining the shadowing effect. As it comes to SARtomographic processing myriad aspect of the problem should be considered, for instance the computational cost and the accuracy for detecting multiple scatterer and elevation resolutions. In this paper the capabilities and advantages of two different methods of SARtomographic processing on real data are compared. Furthermore, the shape and velocity of each building has been attained. The methods include Fourier-based method and Nonlinear Least-Square (NLS). Results show that NLS could provide a good accuracy in elevation. Nonetheless one needs to have a prior knowledge about the model order. In other word it's a parametric method which need an initial assumption about the number of scatterers in each azimuth-range cell. Model selection, i.e., the estimation of the number of distinct scatterers in a resolution cell, has been shown to be a compulsory requirement for parametric methods. Conversely Fourier-based method is a fast method (low computational cost) but extremely suffers from side lobes due its Non-parametric nature, there is an

initial assumption involved. Either of methods mentioned are single looking methods since we must maintain the azimuth-range resolution. Finally we assess the performance of the methods by comparing the obtained coherence of the two tomographic methods with the results of the conventional PS processing which implemented in SARscape software also the reconstructed façade of the two interfering buildings by NLSM is inspected and compared with the PS. One of the main error sources is un-modeled, e.g., nonlinear-motion which is an interesting topic for further research of author. These phase errors are able to deteriorate the elevation estimates. About the novelty of the research few points should be mentioned briefly. First and foremost, the comparison of two different SARTomography methods is an interesting subject which hasn't been implemented in literature. The comparison between methods and PS is done by three different factors (Coherence, Velocity and Height) which are indicator of high accuracy of the research. Results present high density of Permenent Scattere comparing to conventional PS method. These results can be used in further research for the sake of accurate advanced SAR interferometry which are not available in literature in author's knowledge. Moreover, the image mode of the data is stripmap mode which provide 3-m resolution in azimuth and range resolution. It's the first experiment in Iran which exploit Spaceborn VHR SAR data stacks for Tomography purposes. The data stack contains 42 VHR SAR images which can be called 'Rare Informative VHR SAR data stack'.

5. References

[1] A. Hooper, H. Zebker, P. Segall, and B. Kampes, "A new method for measuring deformation on volcanoes and other natural terrains using InSAR persistent scatterers," Geophys. Res. Lett., vol. 31, no. 23, Dec. 2004.

[2] G. Fornaro, S. Member, A. Pauciullo, D. Reale, S. Verde, and S. Member, "Multilook SAR Tomography for 3-D Reconstruction and Monitoring of Single Structures Applied to COSMO-SKYMED Data," vol. 7, no. 7, pp. 2776–2785, 2014.

[3] R. Bamler and M. Eineder, "Accuracy of Differential Shift Estimation by Correlation and Split-Bandwidth Interferometry for Wideband and Delta-k SAR Systems," IEEE Geosci. Remote Sens. Lett., vol. 2, no. 2, pp. 151–155, Apr. 2005.

[4] M. Eineder, N. Adam, R. Bamler, N. Yague-Martinez, and H. Breit, "Spaceborne Spotlight SAR Interferometry With TerraSAR-X," IEEE Trans. Geosci. Remote Sens., vol. 47, no. 5, pp. 1524–1535, May 2009.

[5] A. Ferretti, C. Prati, and F. Rocca, "Permanent scatterers in SAR interferometry," IEEE Trans. Geosci. Remote Sens., vol. 39, no. 1, pp. 8–20, 2001.

[6] S. Gernhardt, N. Adam, M. Eineder, and R. Bamler, "Potential of very high resolution SAR for persistent scatterer interferometry in urban areas," Ann. GIS, vol. 16, no. 2, pp. 103–111, Aug. 2010.

[7] D. W. Vasco, A. Ferretti, and F. Novali, "Estimating permeability from quasi-static deformation: Temporal variations and arrival-time inversion," GEOPHYSICS, vol. 73, no. 6, pp. O37–O52, Nov. 2008.

[8] A. Ferretti, A. Fumagalli, F. Novali, C. Prati, F. Rocca, and A. Rucci, "A New Algorithm for Processing Interferometric Data-Stacks: SqueeSAR," IEEE Trans. Geosci. Remote Sens., vol. 49, no. 9, pp. 3460–3470, Sep. 2011.

[9] Xiao Xiang Zhu, N. Adam, R. Brcic, and R. Bamler, "Space-borne high resolution SAR tomography: experiments in urban environment using TS-X Data," in 2009 Joint Urban Remote Sensing Event, 2009, pp. 1–8.

[10] J. C. Curlander and R. N. McDonough, Synthetic aperture radar : systems and signal processing. Wiley, 1991.

[11] R. F. Hanssen, Radar interferometry : data interpretation and error analysis. .

[12] D. Reale, G. Fornaro, A. Pauciullo, X. Zhu, and R. Bamler, "Tomographic Imaging and Monitoring of Buildings With Very High Resolution SAR Data," IEEE Geosci. Remote Sens. Lett., vol. 8, no. 4, pp. 661–665, Jul. 2011.

[13] X. X. Zhu and R. Bamler, "Demonstration of Super-Resolution for Tomographic SAR Imaging in Urban Environment," IEEE Trans. Geosci. Remote Sens., vol. 50, no. 8, pp. 3150–3157, Aug. 2012.

[14] P. Pasquali et al., "A 3-D SAR experiment with EMSL data," in 1995 International Geoscience and Remote Sensing Symposium, IGARSS '95. Quantitative Remote Sensing for Science and Applications, vol. 1, pp. 784–786.

[15] G. Fornaro, F. Serafino, and F. Soldovieri, "Three-dimensional focusing with multipass SAR data," IEEE Trans. Geosci. Remote Sens., vol. 41, no. 3, pp. 507–517, Mar. 2003.

[16] J. Capon, “High-resolution frequency-wavenumber spectrum analysis,” Proc. IEEE, vol. 57, no. 8, pp. 1408–1418, 1969.

[17] A. Ferretti, M. Bianchi, C. Prati, and F. Rocca, “Higher-order permanent scatterers analysis,” EURASIP J. Appl. Signal Processing, vol. 2005, no. 20, pp. 3231–3242, 2005.

[18] M. Shahzad, S. Member, X. X. Zhu, and S. Member, “Automatic Detection and Reconstruction of 2-D / 3-D Building Shapes From Spaceborne TomoSAR Point Clouds,” pp. 1–19, 2015.

[19] X. X. Zhu and R. Bamler, “Let’s Do the Time Warp: Multicomponent Nonlinear Motion Estimation in Differential SAR Tomography,” IEEE Geosci. Remote Sens. Lett., vol. 8, no. 4, pp. 735–739, Jul. 2011.

[20] A. Ferretti, C. Prati, and F. Rocca, “Nonlinear subsidence rate estimation using permanent scatterers in differential SAR interferometry,” IEEE Trans. Geosci. Remote Sens., vol. 38, no. 5, pp. 2202–2212, 2000.

[21] C. Colesanti, A. Ferretti, F. Novali, C. Prati, and F. Rocca, “Sar monitoring of progressive and seasonal ground deformation using the permanent scatterers technique,” IEEE Trans. Geosci. Remote Sens., vol. 41, no. 7, pp. 1685–1701, Jul. 2003.

[22] F. Lombardini, M. Montanari, and F. Gini, “Reflectivity estimation for multibaseline interferometric radar imaging of layover extended sources,” IEEE Trans. Signal Process., vol. 51, no. 6, pp. 1508–1519, Jun. 2003.

[23] F. Gini, F. Lombardini, and M. Montanari, “Layover solution in multibaseline SAR interferometry,” IEEE Trans. Aerosp. Electron. Syst., vol. 38, no. 4, pp. 1344–1356, Oct. 2002.